ANALYSIS OF A 3D HEAT TRANSFER OF MAGNETOHYDRODYNAMICS $Cu - H_2O$ AND $Al_2O_3 - H_2O$ NANOFLUID OVER AN EXPONENTIALLY STRETCHING PLATE

CELESTINE C. RUTTO (B.ED SCIENCE)

I56/CE/28166/2018

A RESEARCH PROJECT SUBMITTED IN PARTIAL FULFILMENT OF THE REQUIREMENTS FOR THE AWARD OF THE DEGREE OF MASTERS OF SCIENCE (APPLIED MATHEMATICS) IN THE SCHOOL OF PURE AND APPLIED SCIENCES OF KENYATTA UNIVERSITY

NOVEMBER 2024

DECLARATION

Declaration by the Candidate

This project is my original work and has not been submitted for any award of a degree in any University.

Name: Celestine C. Rutto

Signature: .....

Date: .....

Declaration by the Supervisor

This project has been submitted for examination with my approval as the University

Name: Dr. Chepkwony Isaac

Signature: .....

Date: .....

Department of Mathematics and Actuarial Science, Kenyatta University.

ACKNOWLEDGEMENT

I acknowledge God for the journey so far and for all the victories won on the way.

ABSTRACT

Biomedical sensors, such as eye-imaging systems, and drug delivery mechanisms, heavily rely on magnetohydrodynamic (MHD) flow for effective operation. This study investigates the heat transfer characteristics in MHD nanofluid flow over an exponentially stretching surface, focusing on copper (Cu) and alumina (Al_2O_3) nanoparticles suspended in water as the base fluid. The governing equations, which include the continuity, momentum, and energy equations, are formulated under the assumptions of steady, incompressible, and laminar flow. These equations are then made dimensionless using a Similarity Transformation, which reduces the partial differential equations (PDEs) to a system of ordinary differential equations (ODEs). The resulting system is numerically solved using the MATLAB package bvp4c, which is designed for solving boundary value problems. The study emphasises the impact of varying the nanoparticle volume fraction on the rate of heat transfer and skin friction. The results reveal that the Cu-water nanofluid exhibits higher heat transfer rates and lower skin friction compared to the Al_2O_3-water nanofluid, highlighting its potential for enhanced thermal management in biomedical applications.

TABLE OF CONTENTS

LIST OF FIGURES

NOMENCLATURE AND ABBREVIATIONS

Symbol	Meaning	Symbol	Meaning
x, y, z	Distance in three-dimensional space	μ_{nf}	effective nanofluid viscosity
u, v, w	Velocity component in the x, y, z −directions	μ_{bf}	base fluid viscosity
T	Dimensional fluid temperature	μ_{np}	nanoparticle viscosity
T_∞	free stream temperature	ρ_{nf}	effective nanofluid density
T_w	wall temperature	ρ_{bf}	base fluid density
g^*	Acceleration due to gravity	ρ_{np}	nanoparticle density
k^*	mean absorption coefficient	β	Coefficient of thermal expansion
B_0	magnetic field strength	σ_{nf}	effective electrical conductivity
c_p	Specific heat capacity	k_{nf}	effective nanofluid thermal conductivity
σ^*	Stefan–Boltzmann constant	α_{nf}	effective nanofluid thermal diffusivity
ϕ	nanoparticle volume fraction		

Abbreviations	Meaning
MF	Magnetic field
ESS	Exponentially Stretching Surface
MHD	Magnetohydrodynamic

LIST OF ACRONYMS

Acronym	***Meaning***
MF	Magnetic field
RK4-Sh	Runge-Kutta of 4th order with the Shooting Technique
ESS	Exponentially Stretching Surface
BC	Boundary Condition

Chapter 1
INTRODUCTION

1.1 Background

In a search for a fluid with superior thermal and electrical conductivity, Maxwell (1873) came up with the idea of mixing solid particles in the base fluid. Scientists embraced the concepts and successfully added solid particles up to the millimetre scale. The aim of increasing the quality of the base fluid was achieved but issues like clogging and erosion of pipe became prevalent. These issues were theoretically addressed when Choi and Eastman (1995) came up with the notion of dispersion of nanoparticles in the fluid instead of millimetre-sized particles and named such mixture as nanofluid. With the advancement in nanotechnology, remarkable progress has been recorded in the preparation and applications of nanofluids. Applications of nanofluids have taken the front row in engineering and industrial applications such as in recovery of oil wells (McElfresh *et al.*, 2012; Seethamahalakshmi et al., 2024), recovery of waste heat (Khan et al., 2024; Olabi *et al.*, 2021), in heat transfer coolants for microchips, in heat exchangers for car radiators (Rutto et al., 2024; Oke *et al.*, 2021). The thermal and electrical property of any fluid is also further enhanced when the flow takes place under a magnetically influenced condition.

Techniques used in the preparation of nanofluids are continuously being reviewed. As of now, one method is economical but cannot keep the nanoparticles suspended for too long, another method is not economical but it can keep the suspension longer. This is the reason many researchers are involved in trying to come up with best technique. Longevity of suspension depends on several factors ranging from the material from which the nanoparticle was made to the nanoparticle volume fraction, sizes and shapes. Copper Cu,

Copper (II) oxide CuO, Alumina Al_2O_3, Titanium oxide TiO etc. are some of the most reliable metal nanoparticles. Further more, the thermal, electrical and optical properties of the materials are superior at nanoscale compared to the original materials from which they are made. The superiority of the thermal and electrical properties of the nanoparticles contributes to the exceptional performance of nanofluids compared to fluid.

The passage of a fluid with electrical conductivity in a MF produces an electric current inducing a MF; the cycle continues in loop. Lorenz force is generated and it impedes the flow of the fluid. It is of practical significance to consider how MF strength affects the flow of such fluid. The study of magnetohydrodynamic (MHD) flow of nanofluid is of prime importance in biomedical applications, astrophysics, liquid metal flows, and so on.

1.2 Definitions

Nanoparticle: particle whose size is within the nanometre scale is called nanoparticle

Nanofluid: A suspension of nanoparticle in a fluid is called nanofluid.

Magnetohydrodynamic: The branch of fluid mechanics that deals with the flow of fluid in a magnetic field is called magnetohydrodynamic.

No-slip condition: This is the condition that ensures that the fluid layer on a surface travel at the same speed as the surface.

Free Stream: The free stream is the region, far away from surface, where the impact of viscosity is not significant.

Boundary Layer: This is the region in the flow where viscosity effect is very significant.

1.3 Statement of the Problem

We consider the flow of two conducting nanofluids and compare them as they flow over an exponentially stretching surface (ESS). The nanofluids are Cu-H_2O and Al_2O_3-H_2O nanofluids. The surface under consideration is stretched at an exponential rate. By varying volume fraction, we investigate the rate of heat transfer. This project shall investigate the significance of using Cu and/or Al_2O_3 as the nanoparticle in the magnetohydrodynamic flow of water-based nanofluid over an ESS in three dimensions. The impacts of nanoparticle volume fraction and the nanoparticle material on flow parameters shall be investigated.

1.4 Justification

It is no longer new to say that the study of MHD nanofluid has brought about many advancements in science and technology. For this reason, MHD flow has received a lot of attentions from scientists and researchers. Despite the increased emphasis on MHD flow, none of the previous scientific research found in literature has placed emphasis on comparing the heat transfer rate of MHD $Cu - H_2O$ and $Al_2O_3 - H_2O$ nanofluid flow. This study is therefore raised to fill this research gap.

1.5 Objectives

1.5.1 General Objective

This study investigates the heat transfer in magnetohydrodynamic flow of $Cu - H_2O$ and $Al_2O_3 - H_2O$ nanofluid over an exponentially stretching plate.

1.5.2 Specific Objectives

The specific objectives of this study are to;

i. formulate the governing equations for the flow of $Cu - H_2O$ and $Al_2O_3 - H_2O$ nanofluids over an exponentially stretching plate.
ii. nondimensionalise the governing equations using appropriate similarity variables.
iii. determine the heat transfer rates in the magnetohydrodynamic flows of $Cu - H_2O$ and $Al_2O_3 - H_2O$ nanofluids.
iv. find the effect of magnetic field intensity and nanoparticle volume fraction on the $Cu - H_2O$ and $Al_2O_3 - H_2O$ nanofluid magnetohydrodynamic flow over an ESS.

1.6 Significance

Applications of MHD nanofluid include recovery of oil wells, recovery of waste heat, heat transfer coolants for microchips, and heat exchangers for car radiators. This study shall give valuable information to the industries on the choice of nanoparticle required for their processes. Furthermore, this study shall identify the best nanoparticle volume fraction required to enhance heat transfer rate and reduce shear drag.

Chapter 2
LITERATURE REVIEW

Nanoparticles are particles whose sizes are below $100nm$ and a base fluid is the fluid in which a nanoparticle is suspended. Choi and Eastman (1995) referred to the suspension of a nanoparticle in some fluid as ***nanofluid***. Nanofluid has gained attentions from scientists globally and it has been studied extensively, both experimentally and theoretically. More importantly is the attention gained by magnetohydrodynamic nanofluid flow, whose applications have made micro-technology more applicable. Due to the complexity and the huge resources required to prepare nanofluids, it is always safer and cheaper to theoretically and numerically study a certain flow before embarking on the experimental aspect. This explains why there are more of theoretical studies on magnetohydrodynamic flow of nanofluids than there are experimental results (Ali et al., 2023; Malia and Chepkwony, 2019).

Nayak et al. (2019) studied a free convective MHD flow with emphasis on a varying magnetic field strength on three nanofluids with different base fluids. The study compared the heat transfer rate and skin friction of three nanofluids (based on three different base fluids). To advance the studies in magnetohydrodynamics flow of nanofluid, Elazem (2021) numerically explored the significance of MF strength on nanofluid flow when the plate is linearly stretched. The emphasis was on heat and mass transfer rate, which was studied by considering the different viscous dissipation rate, different magnetic field strength, and different Prandtl numbers. A reduction is found in the velocity profiles while the temperature is improved. Irfan *et al.* (2021) focused on the time-dependent thermophysical properties of the flow. Irfan *et al.* (2021) examined the impact of time-

dependent viscosity, time-dependent thermal conductivity, time-dependent surface stretching, and time-dependent wall temperature on a magnetohydrodynamic flow of nanofluid. Noor *et al*. (2021) studied a magnetohydrodynamic flow of Jeffrey nanofluids. The interest of the study is centred on the volume fraction rather than the material from which the nanoparticle was made. The results indicate that raising magnetic field intensity causes retardation in the flow; thereby agreeing with the results of Irfan *et al.* (2021) and Elazem (2021). Most of the previous studies on magnetohydrodynamic flow of nanofluid were considered on a linearly stretching sheet or channel. A forward leap was made by Ahmed and Akbar (2021). Ahmed and Akbar (2021) numerically studied MHD flow of Williamson nanofluid over an ESS, without much emphasis on the nature of the nanoparticles. Haroon et al. (2021) enunciated the effect of uniform MF strength on nanofluid flow in the presence of heat radiation and concluded that the presence of magnetic field hinders fluid flow. Atif et al. (2021) has considered a micropolar-based nanofluid with thermal radiation and mixed convection. The results indicated that the presence of MF boosts flow temperature.

Due to the fact that the material from which nanoparticles have significant effects on the MHD flow nanofluid, this study shall consider a 3D flow of water-based nanofluid in a magnetic field. Comparison is made among two nanoparticles, namely; Cu and Al_2O_3. This focuses on the effects of volume fraction, MF intensity and thermal radiation on magnetohydrodynamic nanofluid flow over an ESS.

Chapter 3
METHODOLOGY

3.1 Formulation of Governing Equations

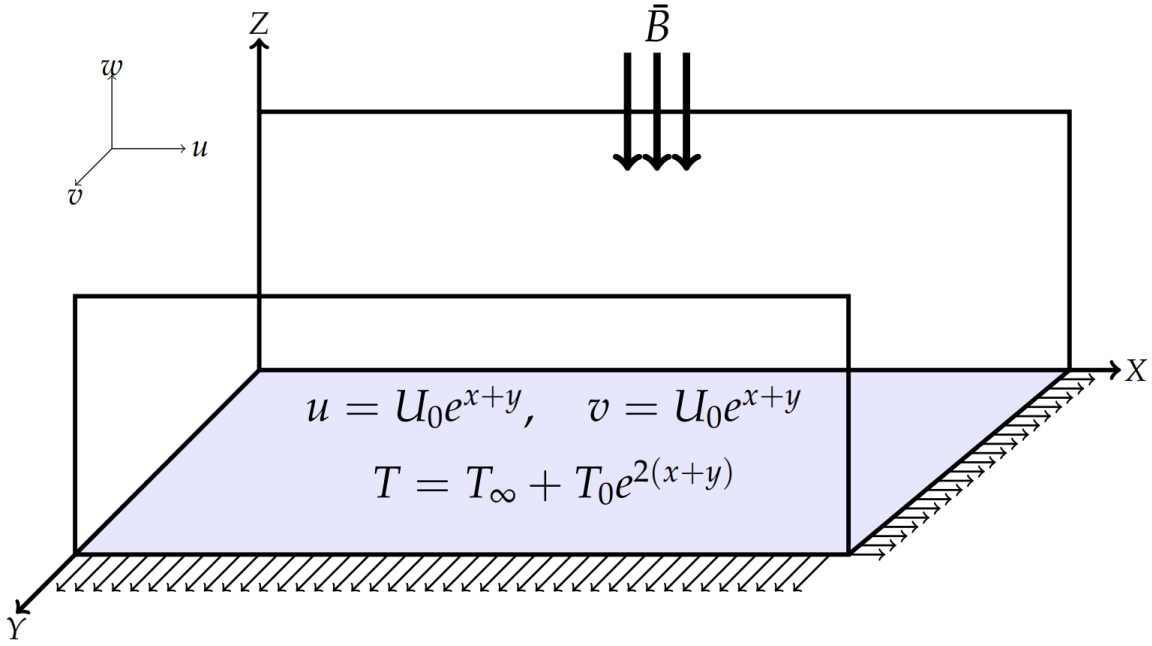

Figure 3.1: Pattern of flow

The pattern shown in Figure (3.1) shows the configuration of the flow to be considered in the project. The flow is steady and in a three-dimensional frame where the magnetic field acts along the z-axis. The nanofluid flows in the x-y plane due to the MF acting at angle 90^o to the flow plane. Since the flow is steady, then the continuity equation is

$$\frac{\partial u}{\partial x} + \frac{\partial v}{\partial y} + \frac{\partial w}{\partial z} = 0.$$

The four Maxwell equations are given as

$$\nabla \times \overleftarrow{\mathbf{E}} = -\frac{\partial \overleftarrow{\mathbf{B}}}{\partial t}, \qquad \nabla \cdot \overleftarrow{\mathbf{E}} = \frac{\rho_c}{\varepsilon_0} \tag{3.1.1}$$

$$\nabla \times \overleftarrow{\mathbf{B}} = \mu_0 \overleftarrow{\mathbf{J}} + \frac{1}{c^2}\frac{\partial \overleftarrow{\mathbf{E}}}{\partial t}, \quad \nabla \cdot \overleftarrow{\mathbf{B}} = 0. \tag{3.1.2}$$

where $\overleftarrow{\mathbf{E}}$ is the electric field intensity, $\overleftarrow{\mathbf{B}}$ is the MF intensity, $\overleftarrow{\mathbf{J}}$ is the current density, and $\mu_0, c, \rho_c, \varepsilon_0$ are the free space permeability, speed of light, charge density, and free space permittivity respectively. The Lorentz force $\overleftarrow{\mathbf{F}}$ is defined as

$$\overleftarrow{\mathbf{F}} = \overleftarrow{\mathbf{j}} \times \overleftarrow{\mathbf{B}}$$

but in magnetically dominant case, the induced current density is given as

$$\overleftarrow{\mathbf{j}} = \sigma \overleftarrow{\mathbf{V}} \times \overleftarrow{\mathbf{B}},$$

where $\overleftarrow{\mathbf{V}} = (u, v, w)$ is the velocity. For a constant MF normal to the flow as shown in the flow configuration (figure 3.1), we have $\overleftarrow{\mathbf{B}} = (0,0, B_0)$. This gives that $\overleftarrow{\mathbf{j}} = (\sigma B_0 v, -\sigma B_0 u, 0)$ and the Lorentz force reduces to

$$\overleftarrow{\mathbf{F}} = (-\sigma B_0^2 u, -\sigma B_0^2 v, 0).$$

Including this in the momentum equations of the Navier Stokes equation, then the momentum equations are

$$uu_x + vu_y + wu_z = \frac{\mu_{nf}}{\rho_{nf}}\frac{\partial^2 u}{\partial z^2} + g^*\beta(T - T_\infty) - \frac{\sigma_{nf} B_0^2 u}{\rho_{nf}}$$

$$uv_x + vv_x + wv_z = \frac{\mu_{nf}}{\rho_{nf}}\frac{\partial^2 w}{\partial y^2} + g^*\beta(T - T_\infty) + \frac{\sigma_{nf} B_0^2 v}{\rho_{nf}}$$

where the left-hand sides represent the convective acceleration, the terms on the RHS represent the viscous term, the buoyancy term and the body force exerted by the magnetic

field respectively. μ_{nf} and ρ_{nf} are the effective dynamic viscosity and effective density defined as

$$\mu_{nf} = (1 + 7.3\phi + 123\phi^2)\mu_{bf},$$

$$\rho_{nf} = (1 - \phi)\rho_{bf} + \phi\rho_{np}.$$

The energy equation is given as

$$u\frac{\partial T}{\partial x} + v\frac{\partial T}{\partial y} + w\frac{\partial T}{\partial z} = \left(\alpha_{nf} + \frac{16\sigma^* T_\infty^3}{3k^*(\rho c_p)_{nf}}\right)\frac{\partial^2 T}{\partial z^2},$$

where the effective thermal diffusivity α_{nf} and specific heat capacity $(\rho c_p)_{nf}$ are defined as

$$\alpha_{nf} = \frac{k_{nf}}{(\rho c_p)_{nf}}, \qquad (\rho c_p)_{nf} = (\rho c_p)_{bf}\left(1 - \phi + \phi\frac{(\rho c_p)_{np}}{(\rho c_p)_{bf}}\right) \tag{3.1.3}$$

$$\begin{aligned} k_{nf} = k_{bf}\Big[&\Big(k_{np} + 2k_{bf} - 2\phi\big(k_{bf} - k_{np}\big)\Big)k_{np} + 2k_{bf} \\ &+ \phi\big(k_{bf} - k_{np}\big)\Big]. \end{aligned} \tag{3.1.4}$$

For an exponentially stretching surface in the x- and y-directions, the boundary conditions are given as follows;

$$at \quad z = 0, \quad \begin{cases} u = U_w = U_0\exp(x + y), \\ v = V_w = U_0\exp(x + y), \\ w = 0, \\ T = T_w = T_\infty + T_0\exp(2x + 2y) \end{cases} \tag{3.1.5}$$

$$as \quad z \to \infty, \quad \begin{cases} u \to 0, \\ v \to 0, \\ T \to T_\infty, \end{cases} . \tag{3.1.6}$$

Hence, the equations governing the 3D MHD nanofluid flow over an ESS in the presence of thermal radiation are

$$\frac{\partial u}{\partial x}+\frac{\partial v}{\partial y}+\frac{\partial w}{\partial z}=0 \tag{3.1.7}$$

$$u\frac{\partial u}{\partial x}+v\frac{\partial u}{\partial y}+w\frac{\partial u}{\partial z}=\frac{\mu_{nf}}{\rho_{nf}}\frac{\partial^2 u}{\partial z^2}+g^*\beta(T-T_\infty)-\frac{\sigma_{nf}B_0^2 u}{\rho_{nf}} \tag{3.1.8}$$

$$u\frac{\partial v}{\partial x}+v\frac{\partial v}{\partial y}+w\frac{\partial v}{\partial z}=\frac{\mu_{nf}}{\rho_{nf}}\frac{\partial^2 w}{\partial y^2}+g^*\beta(T-T_\infty)+\frac{\sigma_{nf}B_0^2 v}{\rho_{nf}} \tag{3.1.9}$$

$$u\frac{\partial T}{\partial x}+v\frac{\partial T}{\partial y}+w\frac{\partial T}{\partial z}=\left(\alpha_{nf}+\frac{16\sigma^*T_\infty^3}{3k^*\left(\rho c_p\right)_{nf}}\right)\frac{\partial^2 T}{\partial z^2}, \tag{3.1.10}$$

with the BCs

$$at\ \ z=0,\ \ \begin{cases}u=U_w=U_0\exp(x+y),\\ v=V_w=U_0\exp(x+y),\\ w=0,\\ T=T_w=T_\infty+T_0\exp(2x+2y)\end{cases} \tag{3.1.11}$$

$$as\ \ z\to\infty,\ \ \begin{cases}u\to 0,\\ v\to 0,\\ T\to T_\infty,\end{cases}. \tag{3.1.12}$$

The factors of engineering applications are the skin frictions and the heat transfer rates;

$$Cf_x=\frac{\tau_x}{\rho_{nf}U_w^2},\quad Cf_z=\frac{\tau_y}{\rho_{nf}U_w^2},\quad and\quad Nu=\frac{zq_w}{\kappa_{nf}(T_w-T_\infty)}. \tag{3.1.13}$$

respectively where the shear stress τ is

$$\tau_x=\mu_{nf}\left.\frac{\partial u}{\partial z}\right|_{z=0}\quad and\quad \tau_z=\mu_{nf}\left.\frac{\partial v}{\partial z}\right|_{z=0}. \tag{3.1.14}$$

and the heat flux q_w is

$$q_w = -\kappa_{nf}\frac{\partial T}{\partial y}\Big|_{z=0}. \tag{3.1.15}$$

3.2 Nondimensionalisation

The system of partial differential equations (3.1.7 – 3.1.10) is a highly nonlinear system that cannot be solved analytically using any of the known analytical methods. The best attempt to having a closed form solution for the system is the use of semi-analytic methods which require a lot of computer resources. In this study, we adopt the use of numerical method to solve the model. For the model to be solvable using the chosen numerical method, the system of partial differential equations (3.1.7 - 3.1.10), along with its boundary and initial conditions (3.1.11 - 3.1.12), is required to be reduced to a system of ODEs. We use the similarity variables

$$\eta = \left(\frac{U_0}{2\nu_{bf}}\right)^{\frac{1}{2}} z\exp\left(\frac{x+y}{2}\right), \quad u = U_0 f'\exp(x+y), \tag{3.2.1}$$

$$v = U_0 g'\exp(x+y), \quad T = T_\infty + \theta T_0\exp(2x+2y) \tag{3.2.2}$$

$$w = -\left(\frac{\nu_{bf}U_0}{2}\right)^{\frac{1}{2}}(f+\eta f'+g+\eta g')\exp\left(\frac{x+y}{2}\right). \tag{3.2.3}$$

From the similarity variables,

$$\frac{\partial \eta}{\partial x} = \frac{\partial \eta}{\partial y} = \frac{1}{2}\left(\frac{U_0}{2\nu_{bf}}\right)^{\frac{1}{2}} z\exp\left(\frac{x+y}{2}\right), \quad and \quad \frac{\partial \eta}{\partial z} = \left(\frac{U_0}{2\nu_{bf}}\right)^{\frac{1}{2}}\exp\left(\frac{x+y}{2}\right),$$

Differentiating u, we have;

$$\frac{\partial u}{\partial x} = \frac{\partial}{\partial x}\left(U_0 f'\exp(x+y)\right) = U_0 f''\exp(x+y)\frac{\partial \eta}{\partial x} + U_0 f'\exp(x+y)$$

$$= U_0 f''\exp(x+y)\cdot\frac{1}{2}\left(\frac{U_0}{2\nu_{bf}}\right)^{\frac{1}{2}} z\exp\left(\frac{x+y}{2}\right) + U_0 f'\exp(x+y)$$

$$= \frac{U_0}{2}\left(\frac{U_0}{2\nu_{bf}}\right)^{\frac{1}{2}} z\exp\left(\frac{3x+3y}{2}\right) f'' + U_0 f'\exp(x+y),$$

and

$$\frac{\partial u}{\partial y} = \frac{\partial}{\partial y}\left(U_0 f'\exp(x+y)\right) = U_0 f''\exp(x+y)\frac{\partial \eta}{\partial y} + U_0 f'\exp(x+y)$$

$$= U_0 f''\exp(x+y)\cdot\frac{1}{2}\left(\frac{U_0}{2\nu_{bf}}\right)^{\frac{1}{2}} z\exp\left(\frac{x+y}{2}\right) + U_0 f'\exp(x+y)$$

$$= \frac{U_0}{2}\left(\frac{U_0}{2\nu_{bf}}\right)^{\frac{1}{2}} z\exp\left(\frac{3x+3y}{2}\right) f'' + U_0 f'\exp(x+y),$$

and

$$\frac{\partial u}{\partial z} = \frac{\partial}{\partial z}\left(U_0 f'\exp(x+y)\right) = U_0 f''\exp(x+y)\frac{\partial \eta}{\partial z}$$

$$= U_0 f''\exp(x+y)\left(\frac{U_0}{2\nu_{bf}}\right)^{\frac{1}{2}}\exp\left(\frac{x+y}{2}\right) = U_0\left(\frac{U_0}{2\nu_{bf}}\right)^{\frac{1}{2}}\exp\left(\frac{3x+3y}{2}\right) f''.$$

and

$$\frac{\partial^2 u}{\partial z^2} = \frac{\partial}{\partial z}\left(U_0\left(\frac{U_0}{2\nu_{bf}}\right)^{\frac{1}{2}}\exp\left(\frac{3x+3y}{2}\right) f''\right)$$

$$= U_0\left(\frac{U_0}{2\nu_{bf}}\right)^{\frac{1}{2}}\exp\left(\frac{3x+3y}{2}\right) f'''\frac{\partial \eta}{\partial z},$$

$$= U_0\left(\frac{U_0}{2\nu_{bf}}\right)^{\frac{1}{2}}\exp\left(\frac{3x+3y}{2}\right) f'''\left(\frac{U_0}{2\nu_{bf}}\right)^{\frac{1}{2}}\exp\left(\frac{x+y}{2}\right)$$

$$= \frac{U_0^2}{2\nu_{bf}} \exp(2x + 2y) f'''.$$

Differentiating v, we have;

$$\frac{\partial v}{\partial x} = \frac{\partial}{\partial x}\left(U_0 g' \exp(x + y)\right) = U_0 g'' \exp(x + y)\frac{\partial \eta}{\partial x} + U_0 g' \exp(x + y)$$

$$= U_0 g'' \exp(x + y) \cdot \frac{1}{2}\left(\frac{U_0}{2\nu_{bf}}\right)^{\frac{1}{2}} z \exp\left(\frac{x + y}{2}\right) + U_0 g' \exp(x + y)$$

$$= \frac{U_0}{2}\left(\frac{U_0}{2\nu_{bf}}\right)^{\frac{1}{2}} z \exp\left(\frac{3x + 3y}{2}\right) g'' + U_0 g' \exp(x + y),$$

and

$$\frac{\partial v}{\partial y} = \frac{\partial}{\partial y}\left(U_0 g' \exp(x + y)\right) = U_0 g'' \exp(x + y)\frac{\partial \eta}{\partial y} + U_0 g' \exp(x + y)$$

$$= U_0 g'' \exp(x + y) \cdot \frac{1}{2}\left(\frac{U_0}{2\nu_{bf}}\right)^{\frac{1}{2}} z \exp\left(\frac{x + y}{2}\right) + U_0 g' \exp(x + y)$$

$$= \frac{U_0}{2}\left(\frac{U_0}{2\nu_{bf}}\right)^{\frac{1}{2}} z \exp\left(\frac{3x + 3y}{2}\right) g'' + U_0 g' \exp(x + y),$$

and

$$\frac{\partial v}{\partial z} = \frac{\partial}{\partial z}\left(U_0 g' \exp(x + y)\right) = U_0 g'' \exp(x + y)\frac{\partial \eta}{\partial z}$$

$$= U_0 g'' \exp(x + y)\left(\frac{U_0}{2\nu_{bf}}\right)^{\frac{1}{2}} \exp\left(\frac{x + y}{2}\right) = U_0\left(\frac{U_0}{2\nu_{bf}}\right)^{\frac{1}{2}} \exp\left(\frac{3x + 3y}{2}\right) g''.$$

and

$$\frac{\partial^2 v}{\partial z^2} = \frac{\partial}{\partial z}\left(U_0\left(\frac{U_0}{2\nu_{bf}}\right)^{\frac{1}{2}}\exp\left(\frac{3x+3y}{2}\right)g''\right) = U_0\left(\frac{U_0}{2\nu_{bf}}\right)^{\frac{1}{2}}\exp\left(\frac{3x+3y}{2}\right)g'''\frac{\partial\eta}{\partial z},$$

$$= U_0\left(\frac{U_0}{2\nu_{bf}}\right)^{\frac{1}{2}}\exp\left(\frac{3x+3y}{2}\right)g'''\left(\frac{U_0}{2\nu_{bf}}\right)^{\frac{1}{2}}\exp\left(\frac{x+y}{2}\right)$$

$$= \frac{U_0^2}{2\nu_{bf}}\exp(2x+2y)g'''.$$

Differentiate w

$$\frac{\partial w}{\partial z} = -\frac{\partial}{\partial z}\left(\left(\frac{\nu_{bf}U_0}{2}\right)^{\frac{1}{2}}(f+\eta f'+g+\eta g')\exp\left(\frac{x+y}{2}\right)\right)$$

$$= -\left(\frac{\nu_{bf}U_0}{2}\right)^{\frac{1}{2}}(f'+\eta f''+f'+g'+\eta g''+g')\frac{\partial\eta}{\partial z}\exp\left(\frac{x+y}{2}\right)$$

$$= -\left(\frac{\nu_{bf}U_0}{2}\right)^{\frac{1}{2}}(f'+\eta f''+f'+g'+\eta g''+g')\left(\frac{U_0}{2\nu_{bf}}\right)^{\frac{1}{2}}\exp\left(\frac{x+y}{2}\right)\exp\left(\frac{x+y}{2}\right)$$

$$= -\frac{U_0}{2}(2f'+\eta f''+2g'+\eta g'')\exp(x+y).$$

Differentiate T,

$$\frac{\partial T}{\partial x} = \frac{\partial}{\partial x}\left(T_\infty+\theta T_0\exp(2x+2y)\right) = T_0\exp(2x+2y)\theta'\frac{\partial\eta}{\partial x} + 2\theta T_0\exp(2x+2y)$$

$$= \frac{1}{2}\left(\frac{U_0}{2\nu_{bf}}\right)^{\frac{1}{2}}z\exp\left(\frac{x+y}{2}\right)T_0\exp(2x+2y)\theta' + 2\theta T_0\exp(2x+2y)$$

and

$$\frac{\partial T}{\partial y} = \frac{\partial}{\partial y}\left(T_\infty+\theta T_0\exp(2x+2y)\right) = T_0\exp(2x+2y)\theta'\frac{\partial\eta}{\partial y} + 2\theta T_0\exp(2x+2y)$$

$$= \frac{1}{2}\left(\frac{U_0}{2\nu_{bf}}\right)^{\frac{1}{2}} z\exp\left(\frac{x+y}{2}\right) T_0\exp(2x+2y)\theta' + 2\theta T_0\exp(2x+2y)$$

and

$$\frac{\partial T}{\partial z} = \frac{\partial}{\partial z}\left(T_\infty + \theta T_0\exp(2x+2y)\right) = \left(\frac{U_0}{2\nu_{bf}}\right)^{\frac{1}{2}} \exp\left(\frac{x+y}{2}\right) T_0\exp(2x+2y)\theta'$$

and

$$\frac{\partial^2 T}{\partial z^2} = \frac{\partial}{\partial z}\left(\left(\frac{U_0}{2\nu_{bf}}\right)^{\frac{1}{2}} \exp\left(\frac{x+y}{2}\right) T_0\exp(2x+2y)\theta'\right) = \frac{U_0}{2\nu_{bf}} T_0\exp(3x+3y)\theta''.$$

In summary,

$$u = U_0 f'\exp(x+y), v = U_0 g'\exp(x+y), T = T_\infty + \theta T_0\exp(2x+2y) \tag{3.2.4}$$

$$w = -\left(\frac{\nu_{bf}U_0}{2}\right)^{\frac{1}{2}} (f + \eta f' + g + \eta g')\exp\left(\frac{x+y}{2}\right), \tag{3.2.5}$$

$$\frac{\partial u}{\partial x} = \frac{\partial u}{\partial y} = \frac{U_0}{2}\left(\frac{U_0}{2\nu_{bf}}\right)^{\frac{1}{2}} z\exp\left(\frac{3x+3y}{2}\right) f'' + U_0 f'\exp(x+y), \tag{3.2.6}$$

$$\frac{\partial u}{\partial z} = U_0\left(\frac{U_0}{2\nu_{bf}}\right)^{\frac{1}{2}} \exp\left(\frac{3x+3y}{2}\right) f'', \quad \frac{\partial^2 u}{\partial z^2} = \frac{U_0^2}{2\nu_{bf}}\exp(2x+2y) f''' \tag{3.2.7}$$

$$\frac{\partial v}{\partial x} = \frac{\partial v}{\partial y} = \frac{U_0}{2}\left(\frac{U_0}{2\nu_{bf}}\right)^{\frac{1}{2}} z\exp\left(\frac{3x+3y}{2}\right) g'' + U_0 g'\exp(x+y) \tag{3.2.8}$$

$$\frac{\partial v}{\partial z} = U_0 \left(\frac{U_0}{2\nu_{bf}}\right)^{\frac{1}{2}} \exp\left(\frac{3x+3y}{2}\right) g'', \qquad \frac{\partial^2 v}{\partial z^2} = \frac{U_0^2}{2\nu_{bf}} \exp(2x+2y) g''' \tag{3.2.9}$$

$$\frac{\partial w}{\partial z} = -\frac{U_0}{2}(2f' + \eta f'' + 2g' + \eta g'')\exp(x+y), \tag{3.2.10}$$

$$\frac{\partial T}{\partial x} = \frac{1}{2}\left(\frac{U_0}{2\nu_{bf}}\right)^{\frac{1}{2}} z\exp\left(\frac{x+y}{2}\right) T_0 \exp(2x+2y)\theta' + 2\theta T_0 \exp(2x+2y) \tag{3.2.11}$$

$$\frac{\partial T}{\partial y} = \frac{1}{2}\left(\frac{U_0}{2\nu_{bf}}\right)^{\frac{1}{2}} z\exp\left(\frac{x+y}{2}\right) T_0 \exp(2x+2y)\theta' + 2\theta T_0 \exp(2x+2y) \tag{3.2.12}$$

$$\frac{\partial T}{\partial z} = \left(\frac{U_0}{2\nu_{bf}}\right)^{\frac{1}{2}} \exp\left(\frac{x+y}{2}\right) T_0 \exp(2x+2y)\theta', \qquad \frac{\partial^2 T}{\partial z^2} = \frac{U_0}{2\nu_{bf}} T_0 \exp(3x+3y)\theta''. \tag{3.2.13}$$

3.2.1 Nondimensionalisation of governing equations

Consider the continuity equation becomes

$$\frac{\partial u}{\partial x}+\frac{\partial v}{\partial y}+\frac{\partial w}{\partial z}=\frac{U_0}{2}\left(\frac{U_0}{2\nu_{bf}}\right)^{\frac{1}{2}}z\exp\left(\frac{3x+3y}{2}\right)f''+U_0f'\exp(x+y)$$

$$+\frac{U_0}{2}\left(\frac{U_0}{2\nu_{bf}}\right)^{\frac{1}{2}}z\exp\left(\frac{3x+3y}{2}\right)g''+U_0g'\exp(x+y)$$

$$-\frac{U_0}{2}(2f'+\eta f''+2g'+\eta g'')\exp(x+y)$$

$$=\left(\frac{U_0}{2}\eta f''+U_0f'+\frac{U_0}{2}\eta g''+U_0g'\right)\exp(x+y)$$

$$-\frac{U_0}{2}(2f'+\eta f''+2g'+\eta g'')\exp(x+y)$$

$$=0$$

From here, it is clear that the similarity variables satisfy the continuity equation. Next is to consider the first momentum equation;

$$u\frac{\partial u}{\partial x}+v\frac{\partial u}{\partial y}+w\frac{\partial u}{\partial z}=\frac{\mu_{nf}}{\rho_{nf}}\frac{\partial^2 u}{\partial z^2}+g^*\beta(T-T_\infty)-\frac{\sigma_{nf}B_0^2u}{\rho_{nf}},$$

then

$$\frac{\partial u}{\partial x}+v\frac{\partial u}{\partial y}+w\frac{\partial u}{\partial z}=U_0f'e^{x+y}\left(\frac{U_0}{2}\left(\frac{U_0}{2\nu_{bf}}\right)^{\frac{1}{2}}ze^{\frac{3x+3y}{2}}f''+U_0f'e^{x+y}\right)$$

$$+U_0g'e^{(x+y)}\left(\frac{U_0}{2}\left(\frac{U_0}{2\nu_{bf}}\right)^{\frac{1}{2}}ze^{\frac{3x+3y}{2}}f''+U_0f'e^{x+y}\right)$$

$$-\left(\frac{\nu_{bf}U_0}{2}\right)^{\frac{1}{2}}(f+\eta f'+g+\eta g')e^{\frac{x+y}{2}}U_0\left(\frac{U_0}{2\nu_{bf}}\right)^{\frac{1}{2}}e^{\frac{3x+3y}{2}}f''$$

$$= U_0^2(f' + g')e^{2x+2y}\left(f' + \frac{\eta}{2}f''\right) - \frac{U_0^2}{2}(f + \eta f' + g + \eta g')e^{2x+2y}f''$$

$$= \left((\eta f'' + 2f')(f' + g') - f''(f + g) - \eta f''(f' + g')\right)\frac{U_0^2}{2}e^{2x+2y}$$

$$u\frac{\partial u}{\partial x} + v\frac{\partial u}{\partial y} + w\frac{\partial u}{\partial z}$$

$$= (2f'(f' + g') - (f + g)f'')\frac{U_0^2}{2}e^{2x+2y} \qquad (3.2.14)$$

and the right-hand side

$$\frac{\mu_{nf}}{\rho_{nf}}\frac{\partial^2 u}{\partial z^2} + g^*\beta(T - T_\infty) - \frac{\sigma_{nf}B_0^2 u}{\rho_{nf}}$$

$$= \frac{\mu_{nf}}{\rho_{nf}}\frac{U_0^2}{2\nu_{bf}}e^{2x+2y}f''' + g^*\beta\theta T_0 e^{2x+2y} - \frac{\sigma_{nf}B_0^2}{\rho_{nf}}U_0 f' e^{x+y}$$

$$= \left(\frac{\mu_{nf}}{\rho_{nf}\nu_{bf}}f''' + \frac{2g^*\beta T_0}{U_0^2}\theta\right.$$

$$\left. - \frac{2\sigma_{nf}B_0^2}{U_0\rho_{nf}e^{x+y}}f'\right)\frac{U_0^2}{2}e^{2x+2y} \qquad (3.2.15)$$

Combining (3.2.14) and (3.2.15), we have

$$\left(2f'^{(f'+g')} - (f + g)f''\right)\frac{U_0^2}{2}e^{2x+2y}$$

$$= \left(\frac{\mu_{nf}}{\rho_{nf}\nu_{bf}}f''' + \frac{2g^*\beta T_0}{U_0^2}\theta - \frac{2\sigma_{nf}B_0^2}{U_0\rho_{nf}e^{x+y}}f'\right)\frac{U_0^2}{2}e^{2x+2y}$$

$$2f'(f' + g') - (f + g)f'' = \frac{\mu_{nf}}{\rho_{nf}\nu_{bf}}f''' + \frac{2g^*\beta T_0}{U_0^2}\theta - \frac{2\sigma_{nf}B_0^2}{U_0\rho_{nf}e^{x+y}}f'$$

$$\frac{\mu_{nf}}{\rho_{nf}\nu_{bf}}f''' + \frac{2g^*\beta T_0}{U_0^2}\theta - \frac{2\sigma_{nf}B_0^2}{U_0\rho_{nf}e^{x+y}}f' - 2f'(f'+g') + (f+g)f'' = 0.$$

On setting the parameters

$$Gr = \frac{g^*\beta T_0}{U_0^2}, \qquad M = \frac{\sigma_{nf}B_0^2}{U_0\rho_{nf}e^{x+y}},$$

then the dimensionless form of first momentum equation is

$$\frac{\mu_{nf}}{\rho_{nf}\nu_{bf}}f''' + 2Gr\theta - 2Mf' - 2f'^{(f'+g')} + (f+g)f'' = 0. \qquad (3.2.16)$$

Next is to consider the second momentum equation;

$$u\frac{\partial v}{\partial x} + v\frac{\partial v}{\partial y} + w\frac{\partial v}{\partial z} = \frac{\mu_{nf}}{\rho_{nf}}\frac{\partial^2 v}{\partial z^2} + g^*\beta(T - T_\infty) + \frac{\sigma_{nf}B_0^2 v}{\rho_{nf}},$$

then

$$\frac{\partial v}{\partial x} + v\frac{\partial v}{\partial y} + w\frac{\partial v}{\partial z} = U_0 f' e^{x+y}\left(\frac{U_0}{2}\left(\frac{U_0}{2\nu_{bf}}\right)^{\frac{1}{2}} z e^{\frac{3x+3y}{2}} g'' + U_0 g' e^{x+y}\right)$$

$$+U_0 g' e^{(x+y)}\left(\frac{U_0}{2}\left(\frac{U_0}{2\nu_{bf}}\right)^{\frac{1}{2}} z e^{\frac{3x+3y}{2}} g'' + U_0 g' e^{x+y}\right)$$

$$-\left(\frac{\nu_{bf}U_0}{2}\right)^{\frac{1}{2}}(f + \eta f' + g + \eta g')e^{\frac{x+y}{2}}U_0\left(\frac{U_0}{2\nu_{bf}}\right)^{\frac{1}{2}} e^{\frac{3x+3y}{2}} g''$$

$$= U_0^2(f'+g')e^{2x+2y}\left(g' + \frac{\eta}{2}g''\right) - \frac{U_0^2}{2}(f + \eta f' + g + \eta g')e^{2x+2y}g'$$

$$= \left((\eta g'' + 2g')(f'+g') - g''^{(f+g)} - \eta g''^{(f'+g')}\right)\frac{U_0^2}{2}e^{2x+2y}$$

$$= \left(2g'(f'+g') - g''(f+g)\right)\frac{U_0^2}{2}e^{2x+2y} \qquad (3.2.17)$$

and the right-hand side

$$\frac{\mu_{nf}}{\rho_{nf}}\frac{\partial^2 v}{\partial z^2} + g^*\beta(T-T_\infty) + \frac{\sigma_{nf}B_0^2 v}{\rho_{nf}}$$

$$= \frac{\mu_{nf}}{\rho_{nf}}\frac{U_0^2}{2\nu_{bf}}e^{2x+2y}g''' + g^*\beta\theta T_0 e^{2x+2y} + \frac{\sigma_{nf}B_0^2}{\rho_{nf}}U_0 g'^{e^{x+y}}$$

$$= \left(\frac{\mu_{nf}}{\rho_{nf}\nu_{bf}}g''' + \frac{2g^*\beta T_0}{U_0^2}\theta - \frac{2\sigma_{nf}B_0^2}{U_0\rho_{nf}e^{x+y}}g'\right)\frac{U_0^2}{2}e^{2x+2y} \qquad (3.2.18)$$

Combining (3.2.17) and (3.2.18), we have

$$\left(2g'(f'+g') - g''(f+g)\right)\frac{U_0^2}{2}e^{2x+2y}$$

$$= \left(\frac{\mu_{nf}}{\rho_{nf}\nu_{bf}}g''' + \frac{2g^*\beta T_0}{U_0^2}\theta + \frac{2\sigma_{nf}B_0^2}{U_0\rho_{nf}e^{x+y}}g'\right)\frac{U_0^2}{2}e^{2x+2y}$$

$$2g'(f'+g') - g''(f+g) = \frac{\mu_{nf}}{\rho_{nf}\nu_{bf}}g''' + \frac{2g^*\beta T_0}{U_0^2}\theta + \frac{2\sigma_{nf}B_0^2}{U_0\rho_{nf}e^{x+y}}g'$$

$$\frac{\mu_{nf}}{\rho_{nf}\nu_{bf}}g''' + \frac{2g^*\beta T_0}{U_0^2}\theta + \frac{2\sigma_{nf}B_0^2}{U_0\rho_{nf}e^{x+y}}g' - 2g'(f'+g') + g''(f+g)$$

$$= 0 \qquad (3.2.19)$$

On setting the parameters

$$Gr = \frac{g^*\beta T_0}{U_0^2}, \qquad M = \frac{\sigma_{nf}B_0^2}{U_0\rho_{nf}e^{x+y}},$$

then the dimensionless form of second momentum equation is

$$\frac{\mu_{nf}}{\rho_{nf}\nu_{bf}}g''' + 2Gr\theta + 2Mg' - 2g'(f' + g') + g''(f + g) = 0 \qquad (3.2.20)$$

Next is to nondimensionalise the energy equation

$$u\frac{\partial T}{\partial x} + v\frac{\partial T}{\partial y} + w\frac{\partial T}{\partial z} = \left(\alpha_{nf} + \frac{16\sigma^* T_\infty^3}{3k^*\left(\rho c_p\right)_{nf}}\right)\frac{\partial^2 T}{\partial z^2},$$

the left-hand side gives

$$u\frac{\partial T}{\partial x} + v\frac{\partial T}{\partial y} + w\frac{\partial T}{\partial z} = U_0 f' e^{x+y}\left(\frac{zT_0}{2}\left(\frac{U_0}{2\nu_{bf}}\right)^{\frac{1}{2}} e^{\frac{5x+5y}{2}}\theta' + 2\theta T_0 e^{2x+2y}\right)$$

$$+U_0 g' e^{x+y}\left(\frac{zT_0}{2}\left(\frac{U_0}{2\nu_{bf}}\right)^{\frac{1}{2}} e^{\frac{5x+5y}{2}}\theta' + 2\theta T_0 e^{2x+2y}\right)$$

$$-\left(\frac{\nu_{bf}U_0}{2}\right)^{\frac{1}{2}}(f + \eta f' + g + \eta g')e^{\frac{x+y}{2}}\left(\frac{U_0}{2\nu_{bf}}\right)^{\frac{1}{2}} T_0 e^{\frac{5x+5y}{2}}\theta'$$

$$= U_0(f' + g')\left(\left(\frac{T_0}{2}\eta\theta' + 2\theta T_0\right) - \frac{U_0 T_0}{2}(f + \eta f' + g + \eta g')\right)e^{3x+3y}\theta'$$

$$= T_0 U_0 e^{3x+3y}\left(2\theta(f' + g') - \frac{1}{2}(f + g)\theta'\right) \qquad (3.2.21)$$

the right-hand side gives

$$\left(\alpha_{nf} + \frac{16\sigma^* T_\infty^3}{3k^*\left(\rho c_p\right)_{nf}}\right)\frac{\partial^2 T}{\partial z^2}$$

$$= \left(\alpha_{nf} + \frac{16\sigma^* T_\infty^3}{3k^*\left(\rho c_p\right)_{nf}}\right)\frac{U_0}{2\nu_{bf}}T_0 e^{3x+3y}\theta'' \qquad (3.2.22)$$

Combining 3.2.21 and 3.2.22, we have

$$T_0U_0e^{3x+3y}\left(2\theta(f'+g')-\frac{1}{2}(f+g)\theta'\right)=\left(\alpha_{nf}+\frac{16\sigma^*T_\infty^3}{3k^*\left(\rho c_p\right)_{nf}}\right)\frac{U_0}{2\nu_{bf}}T_0e^{3x+3y}\theta''$$

$$\left(2\theta(f'+g')-\frac{1}{2}(f+g)\theta'\right)=\left(\alpha_{nf}+\frac{16\sigma^*T_\infty^3}{3k^*\left(\rho c_p\right)_{nf}}\right)\frac{1}{2\nu_{bf}}\theta''$$

$$\left(\alpha_{nf}+\frac{16\sigma^*T_\infty^3}{3k^*\left(\rho c_p\right)_{nf}}\right)\frac{1}{\nu_{bf}}\theta''-4\theta(f'+g')+(f+g)\theta'$$

$$=0. \qquad (3.2.23)$$

Using the effective dynamic viscosity and effective density as

$$\mu_{nf}=(1+7.3\phi+123\phi^2)\mu_{bf}, \qquad \rho_{nf}=(1-\phi)\rho_{bf}+\phi\rho_{np},$$

then,

$$\frac{\mu_{nf}}{\rho_{nf}\nu_{bf}}=\frac{(1+7.3\phi+123\phi^2)\mu_{bf}}{\left((1-\phi)\rho_{bf}+\phi\rho_{np}\right)\nu_{bf}}=\frac{(1+7.3\phi+123\phi^2)\mu_{bf}}{\left(1-\phi+\phi\frac{\rho_{np}}{\rho_{bf}}\right)\rho_{bf}\nu_{bf}}$$

$$=A_1 \qquad (3.2.24)$$

$$\text{where} \quad A_1=\frac{(1+7.3\phi+123\phi^2)}{\left(1-\phi+\phi\frac{\rho_{np}}{\rho_{bf}}\right)},$$

and also,

$$\alpha_{nf}+\frac{16\sigma^*T_\infty^3}{3k^*\left(\rho c_p\right)_{nf}}=\alpha_{nf}+\frac{16\sigma^*T_\infty^3}{3k^*\left(\rho c_p\right)_{nf}}=\alpha_{nf}\left(1+\frac{4}{3}\frac{4\sigma^*T_\infty^3}{k^*\left(\rho c_p\right)_{nf}\alpha_{nf}}\right),$$

meanwhile

$$\alpha_{nf} = \frac{k_{nf}}{(\rho c_p)_{nf}} = \frac{k_{bf}\left[\frac{k_{np}+2k_{bf}-2\phi(k_{bf}-k_{np})}{k_{np}+2k_{bf}+\phi(k_{bf}-k_{np})}\right]}{(1-\phi)(\rho c_p)_{bf}+\phi(\rho c_p)_{np}}$$

$$= \frac{k_{bf}\left[\frac{k_{np}+2k_{bf}-2\phi(k_{bf}-k_{np})}{k_{np}+2k_{bf}+\phi(k_{bf}-k_{np})}\right]}{(\rho c_p)_{bf}\left(1-\phi+\phi\frac{(\rho c_p)_{np}}{(\rho c_p)_{bf}}\right)}$$

$$= \alpha_{bf}A_2,$$

where

$$\alpha_{bf} = \frac{k_{bf}}{(\rho c_p)_{bf}}, \qquad A_2 = \frac{\left[\frac{k_{np}+2k_{bf}-2\phi(k_{bf}-k_{np})}{k_{np}+2k_{bf}+\phi(k_{bf}-k_{np})}\right]}{\left(1-\phi+\phi\frac{(\rho c_p)_{np}}{(\rho c_p)_{bf}}\right)}.$$

The energy equation becomes

$$\left(1+\frac{4}{3}\frac{4\sigma^* T_\infty^3}{k^*(\rho c_p)_{nf}\alpha_{nf}}\right)\frac{\alpha_{nf}}{\nu_{bf}}\theta'' - 4\theta(f'+g') + (f+g)\theta' = 0,$$

and by setting

$$Pr = \frac{\nu_{bf}}{\alpha_{bf}}, \qquad R = \frac{4\sigma^* T_\infty^3}{k^*(\rho c_p)_{nf}\alpha_{nf}},$$

then

$$\left(1+\frac{4}{3}\frac{4\sigma^* T_\infty^3}{k^*(\rho c_p)_{nf}\alpha_{nf}}\right)\frac{\alpha_{bf}A_2}{\nu_{bf}}\theta'' - 4\theta(f'+g') + (f+g)\theta' = 0,$$

$$\left(1+\frac{4}{3}R\right)A_2\theta'' - 4Pr\theta(f'+g') + Pr(f+g)\theta' = 0.$$

3.2.2 Nondimensionalisation of initial-boundary conditions

To start with the initial conditions at $z = 0,\ \eta = 0$;

$$u = U_0 e^{x+y} = U_0 f'^{e^{x+y}} \Rightarrow f' = 1; \quad v = U_0 e^{x+y} = U_0 g'^{e^{x+y}} \Rightarrow g' = 1;$$

$$w = 0 = -\left(\frac{\nu_{bf} U_0}{2}\right)^{\frac{1}{2}} (f + \eta f' + g + \eta g')\exp\left(\frac{x+y}{2}\right) \Rightarrow 0 = f + g;$$

$$T = T_\infty + T_0 e^{2(x+y)} = T_\infty + T_0 \theta e^{2(x+y)} \Rightarrow \theta = 1;$$

and the boundary condition as $z \to \infty,\ \eta \to \infty$;

$$u \to 0 \Rightarrow U_0 f' e^{x+y} \to 0 \Rightarrow f' = 0; \quad v \to 0 \Rightarrow U_0 g' e^{x+y} \to 0 \Rightarrow g' = 0;$$

$$T \to T_\infty \Rightarrow T_\infty + T_0 e^{2(x+y)} \to T_\infty \Rightarrow \theta = 0.$$

Hence, the initial and BCs are

$$f' = 1;\ \ g' = 1;\ \ 0 = f + g;\ \ \theta = 1; \qquad at\ \ \eta = 0,$$

$$f' = 0;\ \ g' = 0;\ \ \theta = 0; \qquad as\ \ \eta \to \infty.$$

3.2.3 Nondimensionalisation of quantities of interest

The horizontal and vertical skin friction and the heat transfer rate defined as

$$Cf_x = \frac{2\tau_x}{\rho_{nf} U_w^2}, \quad Cf_y = \frac{2\tau_y}{\rho_{nf} U_w^2}, \quad \text{and} \qquad Nu = \frac{q_w}{\kappa_{nf}(T_w - T_\infty)}, \qquad (3.2.25)$$

respectively where

$$\tau_x = \mu_{nf}\left.\frac{\partial u}{\partial z}\right|_{z=0} \quad \tau_y = \mu_{nf}\left.\frac{\partial v}{\partial z}\right|_{z=0} \; and \quad q_w$$

$$= -\kappa_{nf}\left.\frac{\partial T}{\partial z}\right|_{z=0}. \qquad (3.2.26)$$

Hence,

$$\tau_x = \mu_{nf}\left.\frac{\partial u}{\partial z}\right|_{z=0} = \mu_{nf}U_0\left(\frac{U_0}{2\nu_{bf}}\right)^{\frac{1}{2}}\exp\left(\frac{3x+3y}{2}\right)f''(0).$$

$$\tau_z = \mu_{nf}\left.\frac{\partial u}{\partial z}\right|_{z=0} = \mu_{nf}U_0\left(\frac{U_0}{2\nu_{bf}}\right)^{\frac{1}{2}}\exp\left(\frac{3x+3y}{2}\right)g''(0).$$

$$q_w = -\kappa_{nf}\left.\frac{\partial T}{\partial z}\right|_{z=0} = -\kappa_{nf}\left(\frac{U_0}{2\nu_{bf}}\right)^{\frac{1}{2}}\exp\left(\frac{x+y}{2}\right)T_0\exp(2x+2y)\theta'(0).$$

With this, the skin frictions become

$$Cf_x = \frac{2\tau_x}{\rho_{nf}U_w^2} = \frac{2\mu_{nf}}{\rho_{nf}(U_0e^{x+y})^2}U_0\left(\frac{U_0}{2\nu_{bf}}\right)^{\frac{1}{2}}\exp\left(\frac{3x+3y}{2}\right)f''(0),$$

$$= \frac{2\mu_{nf}}{\rho_{nf}U_0}\left(\frac{U_0}{2\nu_{bf}}\right)^{\frac{1}{2}}\frac{f''(0)}{\exp\left(\frac{x+y}{2}\right)} = \frac{2A_1\nu_{bf}}{U_0}\left(\frac{U_0}{2\nu_{bf}}\right)^{\frac{1}{2}}\frac{f''(0)}{\exp\left(\frac{x+y}{2}\right)},$$

$$= A_1\left(\frac{2\nu_{bf}}{U_0}\right)^{\frac{1}{2}}\frac{f''(0)}{\exp\left(\frac{x+y}{2}\right)} = A_1Re^{\frac{1}{2}}f''(0) \Rightarrow Re^{-\frac{1}{2}}Cf_x$$

$$= A_1f''(0) \qquad (3.2.27)$$

$$f_y = \frac{2\tau_x}{\rho_{nf}U_w^2} = \frac{2\mu_{nf}}{\rho_{nf}(U_0e^{x+y})^2}U_0\left(\frac{U_0}{2\nu_{bf}}\right)^{\frac{1}{2}}\exp\left(\frac{3x+3y}{2}\right)g''(0)$$

$$= \frac{2\mu_{nf}}{\rho_{nf}U_0}\left(\frac{U_0}{2\nu_{bf}}\right)^{\frac{1}{2}}\frac{g''(0)}{\exp\left(\frac{x+y}{2}\right)} = \frac{2A_1\nu_{bf}}{U_0}\left(\frac{U_0}{2\nu_{bf}}\right)^{\frac{1}{2}}\frac{g''(0)}{\exp\left(\frac{x+y}{2}\right)},$$

$$= A_1\left(\frac{2\nu_{bf}}{U_0}\right)^{\frac{1}{2}}\frac{g''(0)}{\exp\left(\frac{x+y}{2}\right)} = A_1 Re^{\frac{1}{2}}g''^{(0)} \Rightarrow Re^{-\frac{1}{2}}Cf_y = A_1 g''(0). \qquad (3.2.28)$$

$$Nu = \frac{q_w}{\kappa_{nf}(T_w - T_\infty)} = \frac{-\kappa_{nf}\left(\frac{U_0}{2\nu_{bf}}\right)^{\frac{1}{2}}\exp\left(\frac{x+y}{2}\right)T_0\exp(2x+2y)\theta'(0)}{\kappa_{nf}T_0\exp(2x+2y)}$$

$$= -T_0\left(\frac{U_0}{2\nu_{bf}}\right)^{\frac{1}{2}}\frac{\exp\left(\frac{x+y}{2}\right)\theta'(0)}{T_0} = -\left(\frac{U_0}{2\nu_{bf}}\right)^{\frac{1}{2}}\exp\left(\frac{x+y}{2}\right)\theta'(0)$$

$$= -Re^{-\frac{1}{2}}\theta'(0) \Rightarrow Re^{\frac{1}{2}}Nu = \theta'(0) \qquad (3.2.29)$$

3.3 Numerical Method

The dimensionless form of the governing equation is

$$A_1 f''' + 2Gr\theta - 2Mf' - 2f'(f'+g') + f''(f+g) = 0, \qquad (3.3.1)$$

$$A_1 g''' + 2Gr\theta + 2Mg' - 2g'(f'+g') + g''(f+g) = 0, \qquad (3.3.2)$$

$$\left(1+\frac{4}{3}R\right)A_2\theta'' - 4Pr\theta(f'+g') + Pr(f+g)\theta' = 0. \qquad (3.3.3)$$

with the initial and BCs

$$f' = 1;\ \ g' = 1;\ \ 0 = f+g;\ \ \theta = 1; \qquad at\ \ \eta = 0, \qquad (3.3.4)$$

$$f' = 0;\ \ g' = 0;\ \ \theta = 0; \qquad as\ \ \eta \to \infty. \qquad (3.3.5)$$

The dimensionless forms of the quantities of interest are

$$Re^{-1/2}Cf_x = A_1 f''(0);\ \ Re^{-1/2}Cf_y = A_1 g''(0);\ \ Re^{1/2}Nu = \theta'(0).$$

Equations (3.3.1 – 3.3.3) are put as a system of 1st order ODEs

$$\frac{dY_1}{d\eta} = Y_2, \quad \frac{dY_2}{d\eta} = Y_3,$$

$$\frac{dY_3}{d\eta} = -\frac{1}{A_1}\left(2GrY_7 - 2MY_2 - 2Y_2(Y_2 + Y_5) + Y_3(Y_1 + Y_4)\right),$$

$$\frac{dY_4}{d\eta} = Y_5, \quad \frac{dY_5}{d\eta} = Y_6,$$

$$\frac{dY_6}{d\eta} = -\frac{1}{A_1}\left(2GrY_7 + 2MY_5 - 2Y_5(Y_2 + Y_5) + Y_6(Y_1 + Y_4)\right),$$

$$\frac{dY_7}{d\eta} = Y_8,$$

$$\frac{dY_8}{d\eta} = -\frac{1}{\left(1 + \frac{4}{3}R\right)A_2}(-4PrY_4(Y_2 + Y_5) + Pr(Y_2 + Y_4)Y_8).$$

with the conditions

$$X_2(0) = 1; \; X_5(0) = 1; \; X_1(0) + X_4(0) = 0; \; X_7(0) = 1;$$

$$X_2(\infty) = 0; \; X_5(\infty) = 0; \; X_7(\infty) = 0.$$

Two steps are required to solve this ODE system. The first step is the use of Shooting Technique and the second step is the use of Runge-Kutta method.

3.4 Shooting Technique

The system of equations resulting from the nondimensionalisation process comes with Neumann boundary conditions which cannot be used for a numerical procedure. In order to make the system suitable for any numerical procedure, the following steps shall be followed;

STEP 1: Assume initial guesses for the initial conditions.

STEP 2: Solve the equations using the guess values

STEP 3: Check if the solution satisfies the given boundary conditions. If the boundary conditions are satisfied, then the initial guesses are good and the solution has been reached, otherwise repeat steps 1 and 2 to convert the mixed boundary conditions and initial conditions to initial conditions.

3.5 Runge-Kutta (RK) method

The resulting ordinary differential equations from the nondimensionalisation is rewritten as a system of coupled 1st order ODE. The RK scheme of the fourth order shall be used to solve the 1st order ODE. Given the system of first order autonomous ODEs

$$\frac{d}{d\eta}X = F(X),$$

$$X(0) = X_0 \qquad (3.5.1)$$

with

$$X = [X_1, X_2, \cdots, X_n]^T, \qquad F(\eta) = [F_1, F_2, \cdots, F_n]$$

Runge-Kutta scheme of the fourth order is then given as

$$K_1 = hF\left(X^{(m)}\right); \;\; K_2 = hF\left(X^{(m)} + \frac{1}{2}K_1\right)$$

$$K_3 = hF\left(X^{(m)} + \frac{1}{2}K_2\right); \;\; K_4 = hF\left(X^{(m)} + K_3\right)$$

$$X^{(n+1)} = X^{(n)} + \frac{1}{6}(K_1 + 2K_2 + 2K_3 + K_4)$$

Chapter 4
ANALYSIS OF RESULTS AND DISCUSSION

Heat transfer rates and skin friction of copper- and alumina-water nanofluids are investigated and the outcomes are graphically displayed in figures (4.1) and (2). In figures (4.1) and (4.2), Copper-water nanofluid is represented by the black lines while the blue lines represent the alumina-water nanofluid. Each nanofluid is considered under two conditions; low thermal radiation and high thermal radiation. Figure (4.1) shows that heat transfer rates increase with thermal radiation. One can easily observe that copper-water nanofluid possess more heat transfer rate compared with alumina-water. Alumina nanoparticles possess higher specific heat than the copper nanoparticles and this is probably responsible for the lower heat transfer rate in the alumina-water nanofluids. The skin friction is low at low thermal radiation for both copper- and alumina-water nanofluids but high a high thermal radiation (figure (4.2)). A further look at figure (4.2) shows that there is an increased skin friction during the alumina-water nanofluid flow than it is during the copper-water flow. Hence, heat transfer rate is higher in $Cu - H_2O$ nanofluid than the $Al_2O_3 - H_2O$ nanofluid but the skin friction is high in $Al_2O_3 - H_2O$ nanofluid than in $Cu - H_2O$ nanofluid.

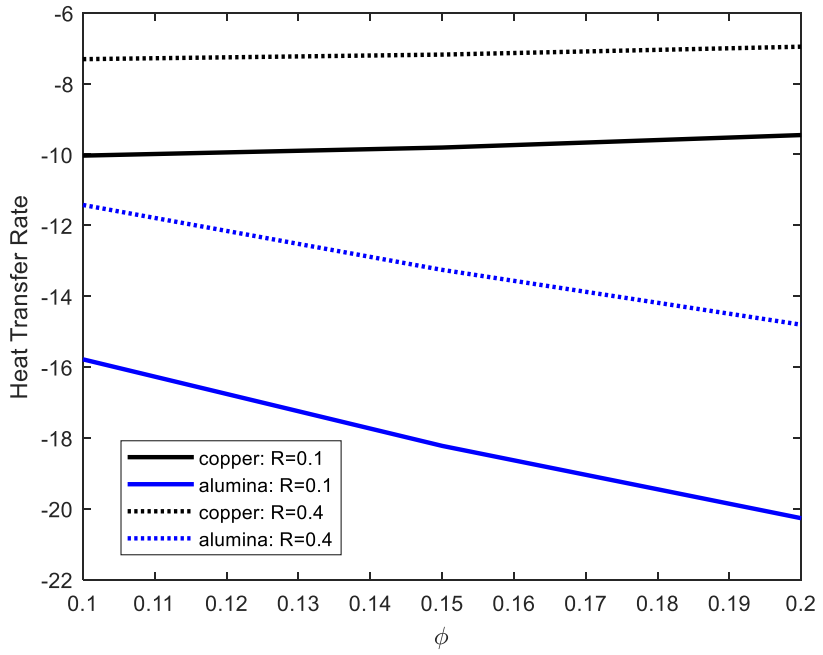

Figure 4.1: Heat transfer rates against ϕ at low and high thermal radiation

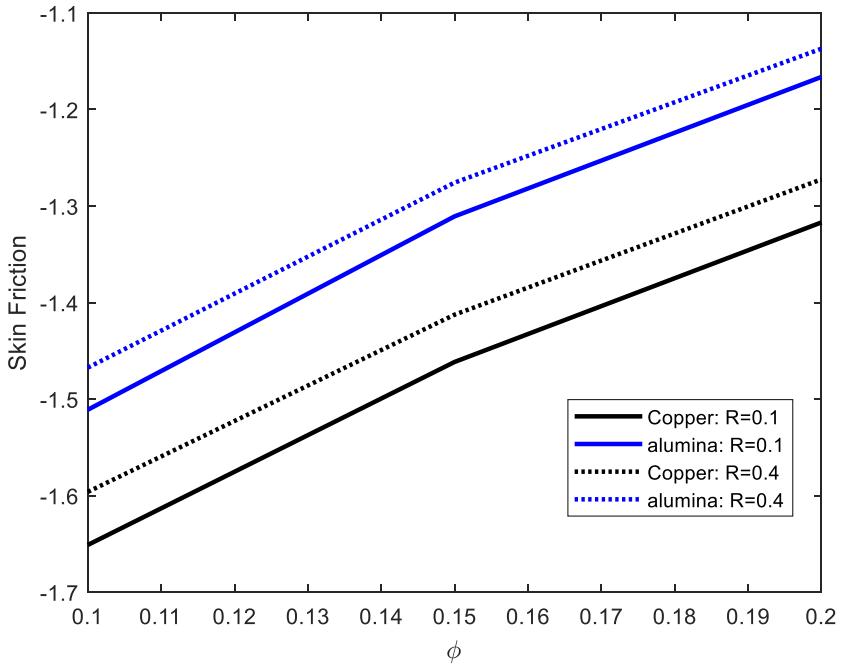

Figure 4.2: Skin friction against ϕ at low and high thermal radiation

In this project, volume fraction represents the ratio of the volume of copper or alumina nanoparticles suspended in a certain volume of water. By varying ϕ, the response of the

velocity and temperature of the flow are analysed and presented in figures (4.3) to (4.5). Suspending more volume of nanoparticles in the fluid can lead to agglomeration which can wear away pipe linings. The alumina nanoparticle possesses lower density compared with the copper nanoparticle, this is probably the reason why the flow velocity is higher in the $Al_2O_3 - H_2O$ nanofluid than the copper-water nanofluid as shown in figures (4.3) and (4.4). By taking a further look at Figures (4.3) and (4.4), it can be generally deduced that the flow velocity is enhanced as the volume fraction is raised. However, flow temperature lowers down as more volume of the nanoparticle as suspended in the base fluid (figure (4.5)).

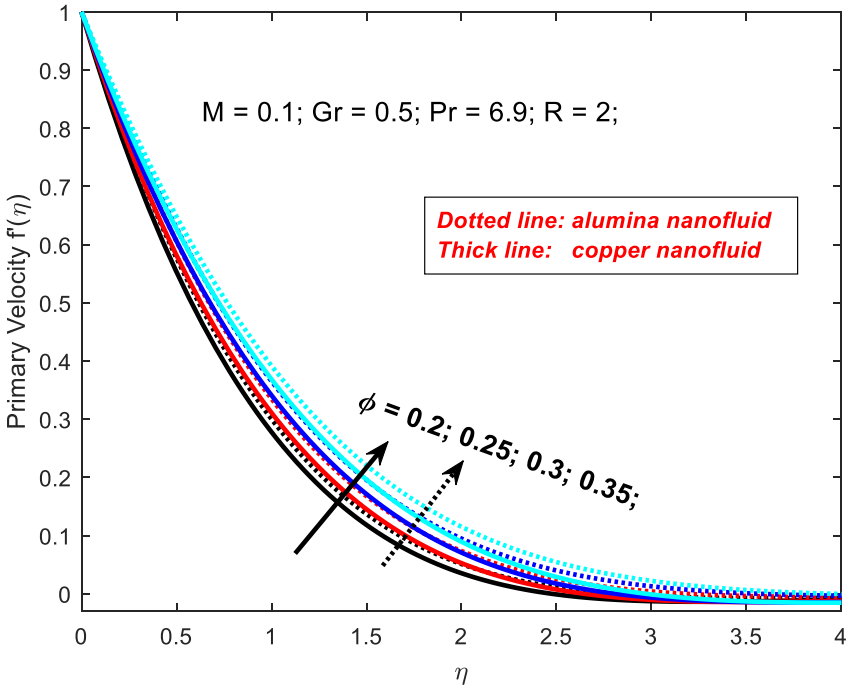

Figure 4.3: Primary velocity against volume fraction

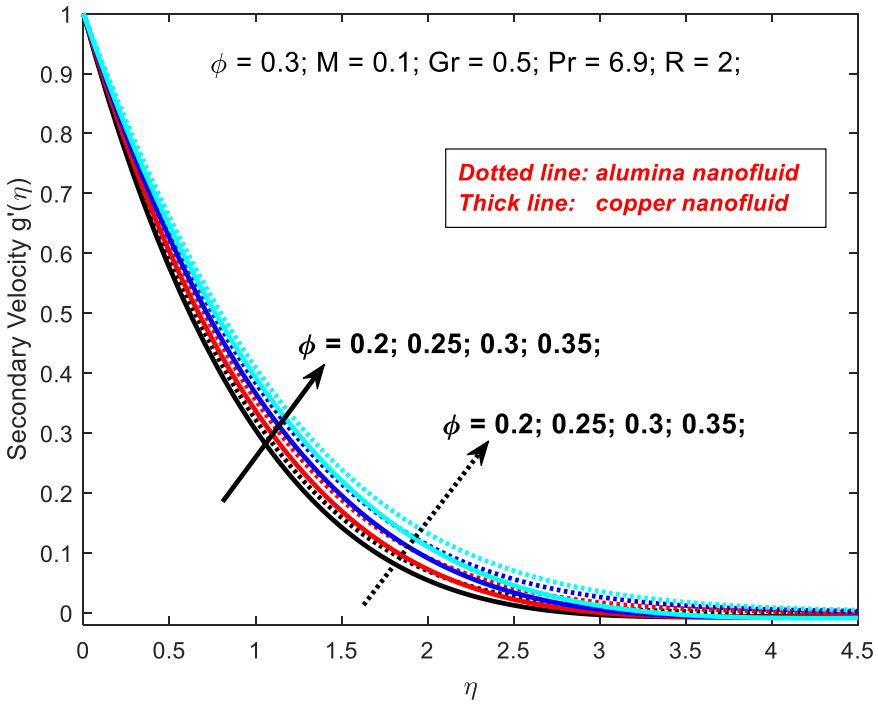

Figure 4.4: Secondary velocity with volume fraction

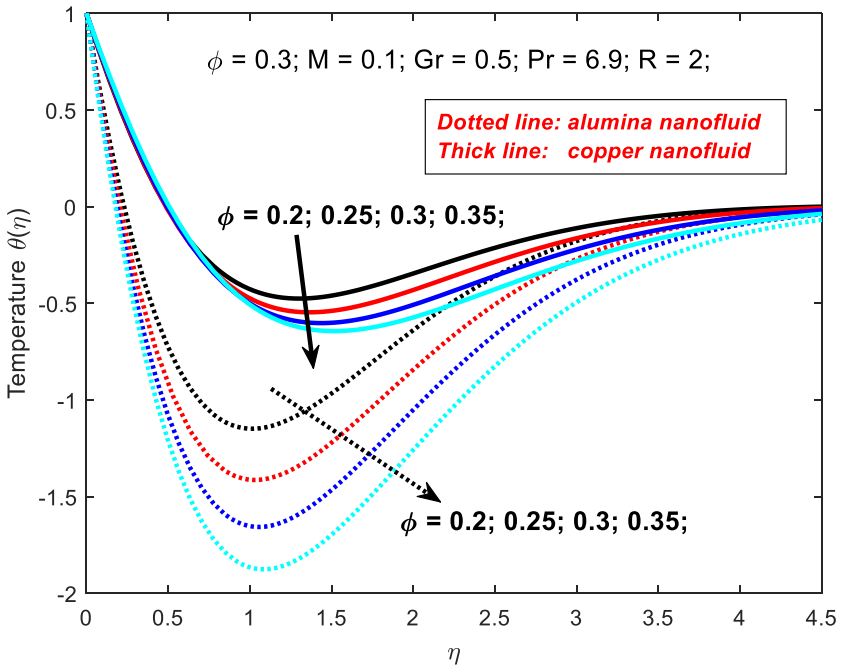

Figure 4.5: Temperature against volume fraction

The effects of MF strength are analysed over the flow of copper-water and alumina-water nanofluids and the results are shown in figures (4.6) to (4.8). Firstly, it is important to note that Lorenz force is produced when a flow takes place in a MF. The Lorenz force acts against the flow and thereby reduces velocity as the magnitude of the MF strength is raised. Just as expected, the velocity profile is reduced as MF strength increases as illustrated in figure (4.6). Due to the opposition caused by the Lorenz force, flow in the secondary direction is enhanced as ϕ increases. Hence, figure (4.7) shows that the secondary velocity increases with increasing MF strength. Also, it is important to note from figure (4.6) and (4.7) that the alumina-water nanofluid flows at higher velocity than the $Cu - H_2O$ nanofluid. $Al_2O_3 - H_2O$ nanofluid possesses higher flow temperature compared to the $Cu - H_2O$ nanofluid (figure (4.8)).

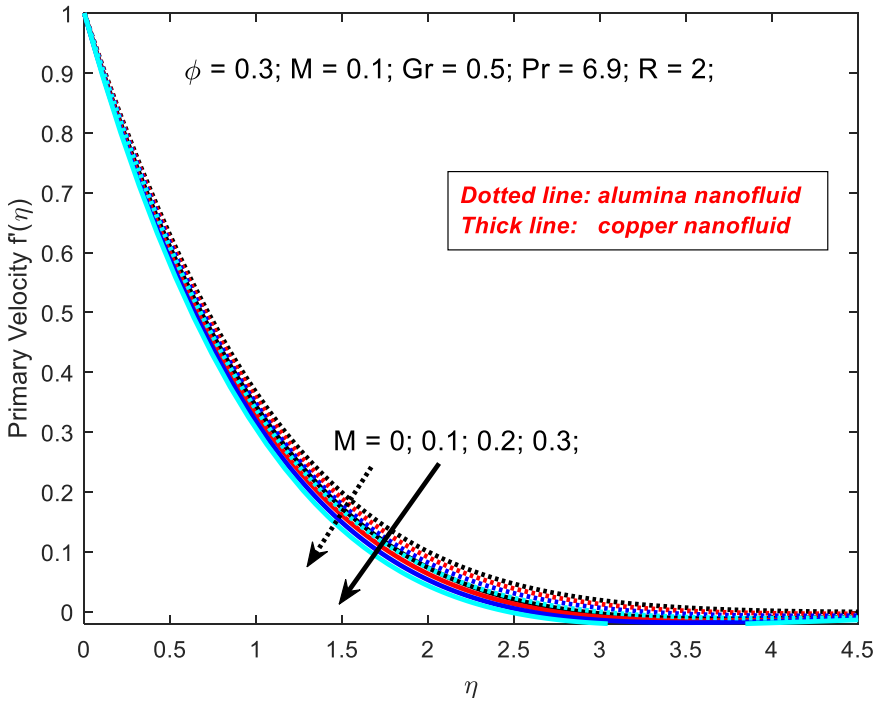

Figure 4.6: Primary velocity with MF

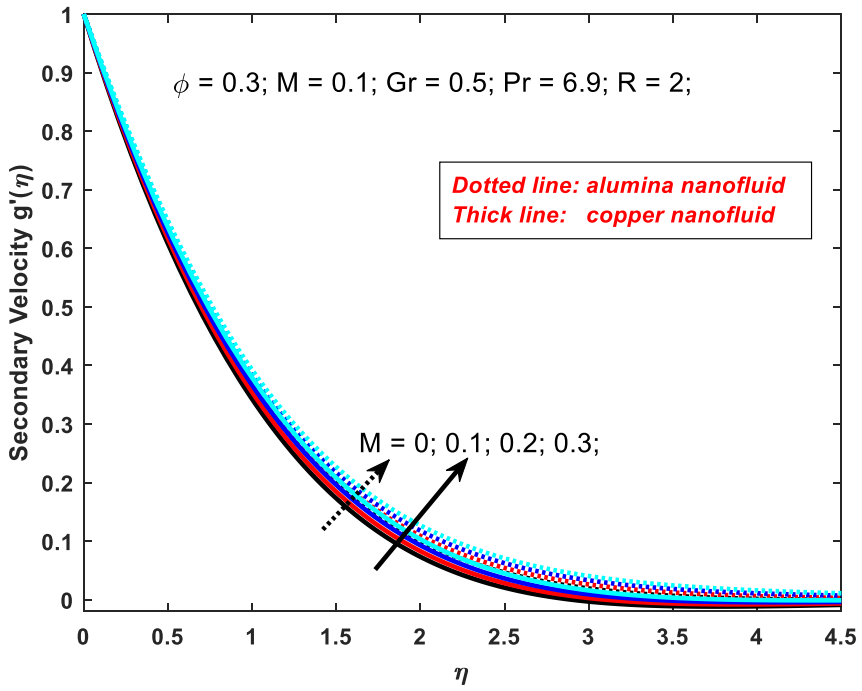

Figure 4.7: Secondary velocity with MF

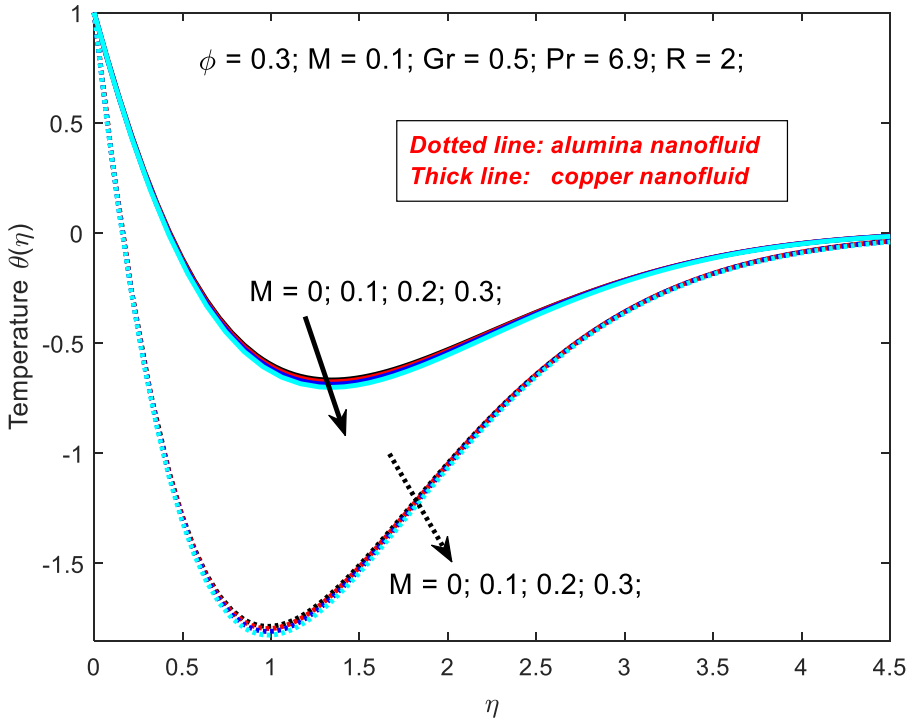

Figure 4.8: Temperature with MF

Chapter 5
CONCLUSION AND RECOMMENDATION

5.1 Conclusion

This study has analysed and discussed the transmission of heat during the flow of copper- and alumina-water nanofluids in a MF. The surface undergoes exponential stretching horizontally while there is an application of thermal radiation normally to the flow. The model is formulated as mathematical equations whose dimensions are removed by the Similarity Variables. Solutions are obtained to the dimensionless equations by employing the RK4-Sh method. The outcomes of this project show that;

1. Heat transfer rates increase with thermal radiation while copper-water nanofluid possess higher heat transfer rate compared with $Al_2O_3 - H_2O$.

2. The skin friction increase with thermal radiation while the skin friction is high in $Al_2O_3 - H_2O$ nanofluid than in $Cu - H_2O$ nanofluid.

3. Flow velocity is enhanced as the volume fraction is raised. Flow velocity is higher in the alumina-water nanofluid than the copper-water nanofluid

4. Flow temperature lowers down as more volume of the nanoparticle as suspended in the base fluid.

5. The primary velocity profile is reduced as MF strength increases while flow in the secondary direction is enhanced as the ϕ increases.

5.2 Recommendations

The flow and heat transfer rate of two nanofluids over an ESS are considered in the presence of a MF and thermal radiation. Based on the outcomes of this study, the following recommendations are made;

1. To increase heat transfer rates, copper-water nanofluid should be considered over the alumina-water nanofluid.

2. To reduce the skin friction in a flow with thermal radiation, copper-water nanofluid should be considered over the alumina-water nanofluid.

3. The flow velocity can be controlled by varying the volume fraction of the nanofluid.

REFERENCES

Ahmed, K. and Akbar, T. (2021). Numerical investigation of magnetohydrodynamics Williamson nanofluid flow over an exponentially stretching surface. *Advances in Mechanical Engineering*, 13(5):16878140211019875.

Ali, B., Ahammad, N. A., Windarto, Oke, A. S., Shah, N. A., & Chung, J. D. (2023). Significance of Tiny Particles of Dust and TiO2 Subject to Lorentz Force: The Case of Non-Newtonian Dusty Rotating Fluid. *Mathematics*, *11*(4), 877.

Atif, S. M., Abbas, M., Rashid, U., and Emadifar, H. (2021). Stagnation Point Flow of EMHD Micropolar Nanofluid with Mixed Convection and Slip Boundary. *Complexity*, 2021(Article ID 3754922).

Choi, S. U. S. and Eastman, J. A. (1995). Enhancing Thermal Conductivity of Fluids with Nanoparticles. *ASME International Mechanical Engineering Congress & Exposition*.

Elazem, N. Y. A. (2021). Numerical results for influence the flow of MHD nanofluids on heat and mass transfer past a stretched surface. *Nonlinear Engineering*, 10(1):28–38.

Haroon, U. R., Islam, R. S., Khan, Z., Alharbi, S. O., Alotaibi, H., and Khan, I. (2021). Impact of Nanofluid Flow over an Elongated Moving Surface with a Uniform Hydromagnetic Field and Nonlinear Heat Reservoir. *Complexity*, 2021(Article ID 9951162).

Irfan, M., Farooq, M. A., Aslam, A., Mushtaq, A., and Shamsi, Z. H. (2021). Magnetohydrodynamic Time-Dependent Bio-Nanofluid Flow in a Porous Medium with Variable Thermophysical Properties. *Mathematical Problems in Engineering*.

Khan, S. U., Adnan, Riaz, A., Ramesh, K., Bhatti, M. M., & Awais, M. (2024). Implicit finite difference simulations for unsteady oscillating flow of Walters-B nanofluid with microbes using the Cattaneo–Christov model. *Numerical Heat Transfer, Part A: Applications*, 1-15.

Malia, M. and Chepkwony, I. (2019). Effects on temperature on applying variable pressure gradient to a magnetohydrodynamic fluid flowing between plates with inclined magnetic field. *Mathematical Theory and Modeling*, 9(11):45–56.

Maxwell, J. C. (1873). A Treatise on Electricity and Magnetism. *Nature*, 7:478–480.

McElfresh, P., Holcomb, D., and Ector, D. (2012). Application of Nanofluid Technology to Improve Recovery in Oil and Gas Wells. *SPE International Oilfield Nanotechnology Conference and Exhibition*. SPE-154827-MS.

Nayak, M. K., Shaw, S., and Chamkha, A. J. (2019). 3D MHD Free Convective Stretched

Flow of a Radiative Nanofluid Inspired by Variable Magnetic Field. *Arab J. Sci. Eng.*, 44:1269–1282.

Noor, N. A. M., Shafie, S., and Admon, M. A. (2021). Heat and mass transfer on MHD squeezing flow of Jeffrey nanofluid in horizontal channel through permeable medium. *PloS one*, 16(5).

Oke, A. S., Animasaun, I. L., Mutuku, W. N., Kimathi, M., Shah, N. A., and Saleem, S. (2021). Significance of Coriolis force, volume fraction, and heat source/sink on the dynamics of water conveying 47nm alumina nanoparticles over a uniform surface. *Chinese Journal of Physics*, 71:716–727.

Olabi, A. G., Elsaid, K., Sayed, E. T., Mahmoud, M. S., Wilberforce, T., Hassiba, R. J., and Abdelkareem, M. A. (2021). Application of nanofluids for enhanced waste heat recovery: A review. *Nano Energy*, 84:105871.

Rutto, C. C., Chepkwony, I., & Oke, A. S. (2024). Numerical Comparison of Cu and Al\(_2\) O\(_3\) Nanoparticles in an MHD Water-based Nanofluid. *Journal of Engineering Research and Reports*, *26*(6), 139-146.

Seethamahalakshmi, V., Rekapalli, L., Rao, T. S., Santoshi, P. N., Reddy, G. V. R., & Oke, A. S. (2024). MHD slip flow of upper-convected Casson and Maxwell nanofluid over a porous stretched sheet: impacts of heat and mass transfer. *CFD Letters*, *16*(3), 96-111.

APPENDIX

Appendix I: MATLAB CODES

```
clc
global A1 A2 Gr M R Pr
phi = 0.3; M = 0.1; Gr = 0.5; Pr = 6.9; R = 2; infty = 7;
rho_bf=997.1; k_bf=0.613; cp_bf=4179; %Water
values = [8933, 400, 385; 3970, 40, 4179]; %[Cu; Al2O3]
j=1; Par_Val = 'M = 0.1; Gr = 0.5; Pr = 6.9; R = 2;';
Values = '\phi = ';
for R = [0.1,0.4]
i=1; Cf=[];Nu=[];
if j==1
lin_sty_1 = 'k-';
lin_sty_2 = 'b-';
lin_sty_3 = 'k-';
lin_sty_4 = 'b-';
elseif j==2
lin_sty_1 = 'k:';
lin_sty_2 = 'b:';
lin_sty_3 = 'k:';
lin_sty_4 = 'b:';
end
for phi = [0.1,0.15,0.2,0.2]
txt = 'Nu';
Values = strcat(Values,string(phi),'; ');
dim_1 = [.5 .6 0.1 .1]; dim_2 = [.3 .5 0.5 .15];
rho_np=values(1,1); k_np=values(1,2); cp_np=values(1,3);
A = A_one(phi,k_bf,k_np,rho_bf,rho_np,cp_bf,cp_np);
A1 = A(1); A2=A(2);
solinit=bvpinit(linspace(0,infty,100),[0 0 0 0 0 0 0 0]);
sol_1= bvp4c(@Fluid,@Bc,solinit);
sol_1.y;
rho_np=values(2,1);
k_np=values(2,2);
cp_np=values(2,3);
A = A_one(phi,k_bf,k_np,rho_bf,rho_np,cp_bf,cp_np);
A1 = A(1); A2=A(2);
solinit=bvpinit(linspace(0,infty,100),[0 0 0 0 0 0 0 0]);
sol_2= bvp4c(@Fluid,@Bc,solinit); sol_2.y;
Cf = [Cf; phi, sol_1.y(3,1), sol_2.y(3,1)];
Nu = [Nu; phi, sol_1.y(8,1), sol_2.y(8,1)];
i = i+1;
end
figure(1), plot(Cf(:,1),Cf(:,2),lin_sty_1,'LineWidth',2)
hold on
figure(1), plot(Cf(:,1),Cf(:,3),lin_sty_2,'LineWidth',2)
xlabel('\phi'), ylabel("Skin Friction")
annotation('textbox',dim_1,'String',Values);
annotation('textbox',dim_2,'String',Par_Val);
hold on
txt_vel = strcat(txt,'_Cf');
saveas(gcf,txt_vel)
figure(2), plot(Nu(:,1),Nu(:,2),lin_sty_3,'LineWidth',2)
hold on
figure(2), plot(Nu(:,1),Nu(:,3),lin_sty_4,'LineWidth',2)
xlabel('\phi'), ylabel("Heat Transfer Rate")
annotation('textbox',dim_1,'String',Values);
annotation('textbox',dim_2,'String',Par_Val);
hold on
txt_vel = strcat(txt,'_Nu');
```

```
saveas(gcf,txt_vel)
j=j+1
end


function res = Fluid(eta,x)
global A1 A2 Gr M R Pr
dx1 = x(2); dx2 = x(3);
dx3 = -(2*Gr*x(7) - 2*M*x(2) -2*x(2)*(x(2)+x(5))...
+ x(3)*(x(1)+x(4)))/A1;
dx4 = x(5); dx5 = x(6);
dx6 = -(2*Gr*x(7) + 2*M*x(5) -2*x(5)*(x(2)+x(5)...
) + x(6)*(x(1)+x(4)))/A1;
dx7 = x(8);
dx8 = -(-4*Pr*x(4)*(x(2)+x(5)) + Pr*(x(2)+x(4))...
*x(8))/(A2*(1+4*R/3));
res = [dx1;dx2;dx3;dx4;dx5;dx6;dx7;dx8];
end

function res = Bc(x0,xinf)
global A1 A2 Gr M R Pr
fw = 0.01;
res = [x0(1)-fw
x0(2)-1
x0(4)+fw
x0(5)-1
x0(7)-1
xinf(2)
xinf(5)
xinf(7)];
end


function res = A_one(phi,k_bf,k_np,rho_bf,rho_np,cp_bf,cp_np)
A11 = 1 + 7.3*phi + 123*phi^2;
A12 = 1 - phi + (rho_np/rho_bf)*phi;
A21=k_np+2*k_bf-2*phi*(k_bf-k_np);
A22=k_np+2*k_bf+phi*(k_bf-k_np);
A23 = 1 - phi + (rho_np*cp_np/(rho_bf*cp_bf))*phi;
res =[A11/A12; A21/(A22*A23)];
end
```